Factors affecting the Cl atom density in a chlorine discharge

Shashank C. Deshmukh and Demetre J. Economou[a)]
Department of Chemical Engineering and Texas Center for Superconductivity, University of Houston, Houston, Texas 77204-4792

(Received 20 December 1991; accepted for publication 23 July 1992)

A mathematical model was developed for the bulk plasma of an electrodeless chlorine discharge sustained in a tubular reactor. The model was used to investigate the factors affecting the Cl atom density in the plasma. Rate coefficients for electron-particle reactions in the Cl_2/Cl mixture were obtained by solving the Boltzmann transport equation for the electron-energy distribution function. These rate coefficients were then used in a plasma model to calculate the self-sustaining electric field, electron density, and atomic chlorine density in the plasma. The effect of frequency, power, gas flow rate, neutral density, tube radius, and wall recombination coefficient was examined. For otherwise identical conditions, nearly the same atom density was obtained in 13.56 MHz and 2.45 GHz discharges. It was found that very high degrees of molecular dissociation are possible with only a few W/cm^3 in the plasma. Despite the fact that the atom density decreased with increasing feed gas flow rate, the atom flux increased with flow rate. In the parameter range investigated, lower pressures and larger tube radii favored higher atom density in the plasma. The model is useful for optimizing source efficiency and for use as a "module" in multidimensional radical transport and reaction models of remote plasma processing reactors.

I. INTRODUCTION

Plasma-enhanced etching and deposition is crucial in microelectronic device fabrication and in materials processing in general.[1] In this process, low-pressure electric gas discharges (plasmas) are used to dissociate a feedstock gas into radicals which react to etch (volatilize) the substrate or to deposit a solid film. Recently, remote plasma-enhanced processing (RPEP) has gained popularity for etching sensitive substrates or for depositing films with tailored properties.[2] In RPEP, a plasma is generated at an upstream location away from the substrate. Reactive radicals generated in the plasma are transported by the flowing gas to the processing chamber where etching or deposition takes place. Examples include etching of polymers with oxygen atoms,[3] etching of silicon with chlorine and hydrogen atoms with or without simultaneous ion bombardment,[4] deposition of Si and its compounds,[5–7] as well as deposition of compound semiconductors.[8] The gas exiting the plasma zone is often mixed with another gas stream to generate a controlled chemical environment over the substrate. Remote plasmas are also used to generate oxygen atoms for *in situ* growth of high-temperature superconducting thin films[9] and for substrate cleaning prior to deposition. In these systems,[2–9] the plasma gas pressure is a few hundred mTorr or greater.

In the applications mentioned above, one is interested in controlling the degree of gas dissociation in the plasma in order to control the radical flux to the substrate. Of the different methods of producing a plasma, excitation at radio frequencies (rf, typically 13.56 MHz) or microwave frequencies (μW, typically at 2.45 GHz) is most common. However, the effect of frequency on plasma kinetics and gas dissociation rates is poorly understood.[10] Earlier studies have considered the effect of frequency on O atom production in oxygen discharges;[11] however, in these studies the electron-energy distribution function was assumed Maxwellian, which is rarely the case. Recent studies have shown that the optimum operating frequency depends on the process under consideration.[12]

In this work a mathematical model was developed of an electrodeless Cl_2 discharge with emphasis on the factors affecting gas dissociation in the plasma. The effect of externally controllable variables, such as power, pressure, flow rate, tube radius, and frequency was studied. In particular, two limiting frequencies were examined: rf at which the electron-energy distribution function (EEDF) was assumed to follow the variations of the field, and μW at which the EEDF cannot follow the field. Because the degree of Cl_2 dissociation can be very high, both molecular and atomic chlorine must be considered in determining the electron kinetics.

II. MATHEMATICAL MODEL

The model considers a chlorine discharge of length L_p sustained in a cylindrical tube (e.g., quartz) of radius R as shown in Fig. 1. Microwave discharges are commonly excited using a resonant cavity.[13] Radio-frequency discharges are capacitively[14] or inductively coupled.[15] For inductively coupled discharges, some capacity coupling is unavoidable unless elaborate screening procedures are followed.[15,16] Gas flows at a predetermined rate and the pressure can be controlled independently. The goal is to determine the degree of gas dissociation as a function of operating conditions including power, pressure, flow rate, and frequency. The approach is as follows: First, the electron transport properties (e.g., mobility and diffusivity) and rate coefficients of reactions involving electrons are determined by

a)Author to whom correspondence should be addressed.

 0021-8979/92/224597-11$04.00

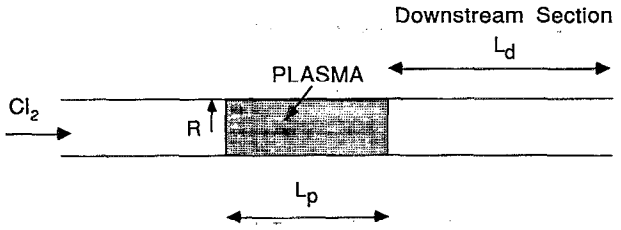

FIG. 1. Schematic of a tubular reactor in which an electrodeless chlorine discharge is sustained.

solving the Boltzmann transport equation for the EEDF. These quantities are then used in mass and energy conservation equations to determine the self-sustained electric field, electron density, and atomic chlorine density in the plasma. In this paper attention is focused on the plasma (source) region. A study of transport and reaction in the downstream region will be reported elsewhere.

A. Electron-energy distribution function

The EEDF is of primary importance in the analysis of gas discharges since it determines the electron transport properties and the rate coefficients for various electron-particle (atom or molecule) reactions. The EEDF depends on the electric field, neutral gas density, excitation frequency, and plasma gas composition. The latter may be quite different than the feedstock gas composition, but this complication is usually not accounted for in plasma modeling works. Since complete dissociation can be achieved readily in a chlorine plasma (see below), the nature of the plasma can change drastically from strongly electronegative (negligible dissociation of Cl_2) to electropositive (high dissociation of Cl_2) as one varies, for example, the power delivered to the plasma. Hence it is important to include the effect of Cl atoms on electron and plasma kinetics.

The time response of the electron velocity distribution function in an ac field is determined by the relative magnitudes of the angular frequency of the applied electric field [$E=E_0\sin(\omega t)$, $\omega=2\pi F$] and the momentum ν_m and energy relaxation frequencies ν_u.[17] When $\omega \gg \nu_u$, the characteristic time for energy relaxation is much greater than the period of the applied field. As a consequence, the EEDF cannot respond to the time variation of the applied field and does not change appreciably over a cycle. When the EEDF is time independent (e.g., for $\omega \gg \nu_u$), neglecting any spatial variations and adopting the two-term expansion, the Boltzmann equation can be written as[18]

$$-\frac{2}{3}\frac{d}{d\epsilon}\left\{\epsilon^{3/2}\nu_m(\epsilon)\left[\frac{e}{m}\frac{E^2}{[\nu_m^2(\epsilon)+\omega^2]}\frac{df}{d\epsilon}+\frac{3m}{M}\left(f(\epsilon)+\frac{kT_g}{e}\frac{df(\epsilon)}{d\epsilon}\right)\right]\right\} = \sum_j [\nu_j(\epsilon+\epsilon_j)f(\epsilon+\epsilon_j)(\epsilon+\epsilon_j)^{1/2} - \nu_j(\epsilon)f(\epsilon)(\epsilon)^{1/2}], \quad (1)$$

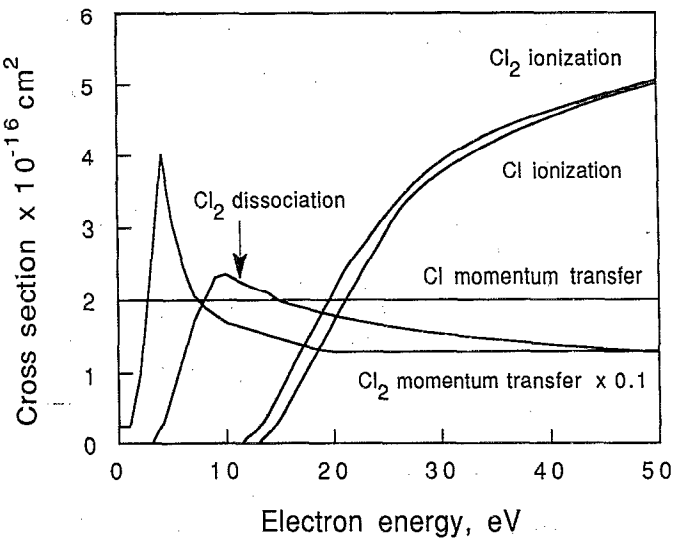

FIG. 2. Selected cross sections for electron-molecule and electron-atom reactions in a Cl_2/Cl mixture.

where ϵ and m are the electron energy and mass, respectively, f is the (isotropic) EEDF, M is the neutral mass, T_g is the gas temperature, ϵ_j is the threshold energy of inelastic process j, and E is the electric field. The collision frequency for inelastic process j is $\nu_j(\epsilon)=N\sigma_j(\epsilon)(2\epsilon e/m)^{1/2}$, $\sigma_j(\epsilon)$ being the collision cross section. Superelastic and electron-electron (EE) collisions are neglected in Eq. (1). The power transferred per electron is given by

$$\frac{P}{n_e}=\frac{e^2}{m}\frac{\nu_m(\epsilon)E^2}{[\nu_m^2(\epsilon)+\omega^2]}, \quad (2)$$

where P is the power and n_e is the electron density. In Eqs. (1) and (2), ν_m is expressed as a function of energy ϵ. It can be shown using Eq. (2) that the power becomes maximum at the resonance condition $\nu_m(\epsilon)=\omega$. Since ν_m is proportional to N, Eq. (1) shows that the EEDF depends on both E/N and E/ω. At the limit $\omega \gg \nu_m(\epsilon)$ the EEDF will be a function of E/ω alone (for a given gas composition). At the other extreme $\omega \ll \nu_m(\epsilon)$ the EEDF will be a function of E/N alone. For the μW case, the EEDF is quasistationary and E in Eq. (1) was taken as the rms field, $E_{\rm rms}=E_0/\sqrt{2}$. For the rf case, the EEDF was assumed to follow the field and E was taken as the dc field [$\omega=0$ in Eq. (1)] corresponding to the instantaneous value of the actual time-varying field.

The cross sections used for the various elastic and inelastic processes for atomic and molecular chlorine were the same as those used by Rogoff, Kramer, and Piejak[19] and Aydil and Economou.[20] Inelastic processes for molecular chlorine included vibrational excitation, ionization, dissociative attachment, and excitation to $B\,^3\Pi$, $2\,^1\Pi$, $2\,^1\Sigma$, and $C\,^1\Pi$ states. Excitation to the $C\,^1\Pi$ state is dissociative and is the main channel producing atomic chlorine. Inelastic processes for atomic chlorine included ionization and excitation to six different electronic states. Selected cross sections are shown in Fig. 2. Table I shows the electron

TABLE I. Important reactions in the chlorine discharge.

Reaction		Threshold (eV)	
Electron-impact reactions:			
Molecular ionization	$Cl_2+e^- \rightarrow Cl_2^+ + 2e^-$	11.5	(R1)
Atomic ionization	$Cl+e^- \rightarrow Cl^+ + 2e^-$	13.0	(R2)
Dissociative attachment	$Cl_2+e^- \rightarrow Cl_2^{-*}$ $\rightarrow Cl + Cl^-$		(R3)
Dissociative excitation	$Cl_2+e^- \rightarrow Cl_2^*(C\,^1\Pi)$ $+ e^- \rightarrow 2Cl + e^-$	3.12	(R4)
Dissociative ionization	$Cl_2+e^- \rightarrow Cl^+ + Cl + 2e^-$	11.5	
Electronic excitation (molecular chlorine)	Cl_2+e^- $\rightarrow Cl_2^*(B\,^3\Pi) + e^-$	2.50	
	$Cl_2+e^- \rightarrow Cl_2^*(2\,^1\Pi$ and $2\,^1\Sigma)+e^-$	9.25	
Vibrational excitation	$Cl_2+e^- \rightarrow Cl{:::}Cl^*+e^-$	0.069	
Electronic excitations (six) (atomic chlorine)	$Cl+e^- \rightarrow Cl^*+e^-$		
Other reactions:			
Ion-ion recombination	$Cl_2^+ + Cl^- \rightarrow Cl_2 + Cl$ $Cl^+ + Cl^- \rightarrow 2Cl$		
Volume recombination	$Cl+Cl+M \rightarrow Cl_2+M$		(R5)
Wall recombination	$Cl+\text{wall} \rightarrow \frac{1}{2}Cl_2+\text{wall}$		(R6)

and neutral particle reactions.

A computer code developed by Luft[21] was used to solve the Boltzmann equation. The solution is based on expanding the distribution function in Legendre polynomials[22] and retaining the first two terms of the expansion. The two-term approximation assumes that the distribution function is essentially isotropic with the anisotropy due to the electric field constituting only a small perturbation to the isotropic equilibrium distribution.

The Boltzmann equation was solved for different combinations of E/N and ω/N. The distribution function was normalized such that

$$\int_0^\infty f(\epsilon)\sqrt{\epsilon}\,d\epsilon = 1. \tag{3}$$

Two excitation frequencies were examined, rf at $F=13.56$ MHz and μW at $F=2.45$ GHz. For given ω/N, the rate coefficients for various electron-particle reactions k_j were fitted as functions of E/N and y_{Cl} (mole fraction of atomic chlorine in the discharge) using the following expression:

$$k_j = (C_1 + C_2 y_{Cl} + C_3 y_{Cl}^2)\exp[-(C_4 + C_5 y_{Cl} + C_6 y_{Cl}^2)/E/N], \tag{4}$$

where C_1 through C_6 are constants. The accuracy of these fits was within 5%–10% over the entire range of E/N examined.

Electron-electron collisions can affect the EEDF especially at high degrees of ionization. For example, the EEDF in an argon discharge is influenced by EE collisions[18] at degrees of ionization $>10^{-4}$. However, EE collisions are not as important in molecular gas plasmas;[18] besides, the degree of ionization in the present case is $<10^{-5}$ (see below). Electron-electron collisions are expected to be important in ECR reactors due to the high degree of ionization obtained in these reactors.

B. Plasma model

A plasma model was developed to predict three key plasma properties, namely, the self-sustaining electric field, the electron density, and the atomic chlorine density. The model is based on the assumption of spatial homogeneity of these three quantites. Let us elaborate on this assumption.

The radical density uniformity depends primarily on the wall reactivity. The radical density is expected to be uniform across the radius of the tube if diffusion is fast enough to alleviate concentration gradients. In quantitative terms, the Thiele modulus $\Phi^2 = k_s R/D_{Cl}$ must be less than unity. Here k_s is the surface recombination rate coefficient, R is the tube radius, and D_{Cl} is the radical diffusivity. For the conditions of our study, $\Phi^2 < 1$ is satisfied for most situations except for unreasonably high wall reactivities.

The plasma homogeneity depends on the electric-field (E) distribution. Indeed E can be nonuniform in both microwave and rf (inductively or capacitively coupled) plasmas.[16,23] However, Ferreira *et al.*[18] have noted that a model based on spatially averaged quantities gives nearly the same results as a more elaborate model which accounts for field inhomogeneities. In fact, the spatially average field approximation has been applied quite successfully at dc, rf, and microwave frequencies.[11,18,24] For chlorine in particular, distributed parameter models for capacitively coupled discharges have shown that the electric field and electron density are very uniform in the bulk plasma.[25]

One can account for plasma nonuniformities but the complexity of the model increases considerably. In this work we were interested in the average radical density in the discharge (to optimize gas dissociation) and not in the electric-field distribution. Our goal was to develop a model that can incorporate complex plasma chemistry yet have minimal CPU time requirements. This model will be useful as a "module" in multidimensional radical transport and reaction models of remote plasma processing reactors.

Table I shows the reactions considered. Electrons are produced by ionization of molecular (reaction R1) and atomic (R2) chlorine and are lost via dissociative attachment (R3) and diffusion to the walls of the tube. Atomic chlorine is produced mainly by dissociative excitation (R4) and also by dissociative attachment, and is lost by volume and wall recombination (R5 and R6, respectively). Electron attachment to atomic chlorine was not considered due to the very low cross section.[26]

In order to determine the three unknown plasma properties three independent equations are required. These are the electron density balance, the Cl density balance, and the power balance.

1. Electron density balance

The electron density balance can be written as

$$\frac{d}{dt}n_e = k_{i1}y_{Cl}Nn_e + k_{i2}(1-y_{Cl})Nn_e - k_a(1-y_{Cl})Nn_e - \frac{D_{se}}{\Lambda^2}n_e. \quad (5)$$

Here k_{i1}, k_{i2}, and k_a are the rate coefficients for atomic ionization, molecular ionization, and attachment, respectively. The terms on the right-hand side (rhs) represent ionization of atomic chlorine, ionization of molecular chlorine, attachment to molecular chlorine, and diffusion to the walls of the container, respectively. D_{se} is an effective electron diffusion coefficient which was taken to be the same as the ambipolar diffusion coefficient, D_a.[27] Chlorine is a highly electronegative gas and the ratio $\alpha = n_-/n_e$ (negative Cl^- ion density to electron density) can be much greater than one. In such cases a generalized equation for the ambipolar diffusion coefficient is needed that accounts for diffusion in the ternary mixture of electrons, positive ions, and negative ions. The equation for D_a used in this work is a simplified form of Eq. (11) given in Ref. 28. Assuming similar values for the diffusivity of positive and negative ions ($D_+ \approx D_-$), D_a can be written as

$$D_a = D_e\frac{(\alpha+\mu_{r+})}{(\alpha+\mu_{re}+\mu_{r+})}, \quad (6)$$

where D_e is the electron diffusivity as determined from the EEDF, $\alpha = n_-/n_e$, $\mu_{re} = \mu_e/(\mu_+ + \mu_-)$, and $\mu_{r+} = \mu_+/(\mu_+ + \mu_-)$. The electron mobility μ_e was also obtained from the EEDF. The positive and negative ion mobilities (μ_+ and μ_-) were taken to be 1.52×10^{19}/N and 1.88×10^{19}/N cm^2/V s, respectively.[29]

The negative ion density was estimated using a steady-state balance for Cl^- ions. If one equates the rate of production of Cl^- by dissociative attachment to their loss by Cl_2^+-Cl^- and Cl^+-Cl^- ion-ion recombination (rate coefficient of recombination reactions $k_{ii} = 5\times10^{-8}$ cm^3/s),[30] n_- can be obtained as

$$n_- = -\frac{n_e}{2} + \left[\left(\frac{n_e}{2}\right)^2 + \frac{k_aN(1-y_{Cl})}{k_{ii}}n_e\right]^{1/2}. \quad (7)$$

The diffusion length Λ for cylindrical geometry is given by

$$\frac{1}{\Lambda^2} = \left(\frac{2.405}{R}\right)^2 + \left(\frac{\pi}{L_p}\right)^2. \quad (8)$$

When the discharge length L_p is much greater than the tube radius R, $\Lambda = R/2.405$.

2. Atomic chlorine density balance

If Q_0 is the feed rate of molecular chlorine (sccm) then the component balance for atomic chlorine can be written as

$$\frac{8.96\times10^{17}Q_0}{V_p}\frac{y_{Cl}}{(2-y_{Cl})} = (k_a+2k_d)N(1-y_{Cl})n_e - 2k_vN^3y_{Cl}^2 - 2\frac{k_s}{R}Ny_{Cl}, \quad (9)$$

where V_p is the plasma volume, y_{Cl} is the mole fraction of atomic chlorine, k_d is the rate coefficient for electron-impact dissociation of molecular chlorine, and k_v is the rate coefficient for volume recombination of atomic chlorine. The left-hand side (lhs) of Eq. (9) is the rate at which atomic chlorine leaves the plasma volume. The first term on the rhs represents the rate of production of Cl by dissociative attachment and dissociation. The second and third terms on the rhs represent the loss rate of Cl by volume recombination and surface recombination on the walls of the discharge tube, respectively. The surface recombination rate coefficient k_s is given by

$$k_s = \frac{\gamma}{4}\left(\frac{8kT}{\pi M_{Cl}}\right)^{1/2}, \quad (10)$$

and γ is the reaction probability, k is the Boltzmann constant, M_{Cl} is the mass of atomic chlorine, and T is the gas temperature. Unless otherwise stated γ was taken as 4×10^{-5},[31] and the volume recombination coefficient was taken as 4.5×10^{-32} cm^6/s.[32]

When the EEDF follows the temporal variations of the field (e.g., rf case), the electron-impact reaction rate coefficients are modulated at twice the excitation frequency. Thus the atomic chlorine production by e-impact dissociation is time dependent. However, volume and wall recombination losses of Cl occur at a time scale much longer than the period of the applied field, resulting in a Cl density that is not modulated in time. Therefore, for the rf case, k_a and k_d in Eq. (9) were time averaged over the period of the applied field.

3. Power balance

The energy absorbed from the field by the electron cloud is lost to elastic and inelastic collisions with the gas particles. At steady state (e.g., μW case) the power balance can be written as

$$\frac{P}{V_p} = \frac{2m}{M}\langle\epsilon\rangle k_m n_e N + \sum_i \epsilon_i k_i (1-y_{Cl})Nn_e + \sum_j \epsilon_j k_j y_{Cl}Nn_e + \langle\epsilon\rangle k_{i1}y_{Cl}Nn_e + \langle\epsilon\rangle k_{i2}(1-y_{Cl})Nn_e, \quad (11)$$

where $\langle\epsilon\rangle$ is the average electron energy (averaged over the EEDF), ϵ_i is the energy loss for the ith inelastic process for molecular chlorine, k_i is the corresponding rate coefficient, and ϵ_j and k_j are the corresponding quantities for atomic chlorine. The first term on the rhs accounts for the rate at which energy is lost by the electrons through elastic collisions. The second and third terms on the rhs represent the rate at which energy is lost via inelastic processes involving molecular and atomic chlorine, respectively. Finally, the fourth and fifth terms represent the rate at which energy is needed to bring the electrons produced by ionization to the average electron energy.

A problem arises in evaluating the power absorbed by the electrons which is the quantity needed in Eq. (11). Part of the total input power is dissipated in the bulk plasma and the rest is dissipated in the sheath. The power dissipated in the sheaths of a capacitively coupled rf diode reactor operating in the same range of pressure and dimensions (electrode spacing in that case) as used for the present model was estimated from the product of the measured ion flux and sheath voltage. It was found that $<10\%$ of the input power was dissipated in each of the two sheaths, i.e., most of the power was dissipated in the bulk plasma.[20] As frequency increases, an even smaller fraction of the power is dissipated in the sheaths. Therefore, sheath effects should be minimal in electrodeless chlorine discharges, especially at microwave frequencies.

Electrons are the main charge carriers. The electron current dominates the ion current at microwave frequencies regardless of the degree of molecular dissociation. At rf frequencies, ions make some contribution especially at low degrees of molecular dissociation for which the electron density is reduced due to attachment. However, even for a Cl mole fraction <0.1, it was estimated that the electron current is a few times higher than the negative ion current. For moderate degrees of gas dissociation, the electron current dominates completely.

III. METHOD OF SOLUTION

For given molecular chlorine feed rate, neutral density (pressure), power, frequency, and discharge tube radius, the balance equations (5), (9), and (11) were solved for the self-sustaining electric field, electron density, and atomic chlorine mole fraction. These equations are coupled through the dependence of the electron-particle reaction rate coefficients on the electric field and the mole fraction of atomic chlorine. The coupled system of equations was solved using the Fortran algorithm DERPAR.[33] The power density was treated as the arc-length continuation parameter.

For the μW case, the lhs of Eq. (5) was set equal to zero since the EEDF is not modulated in time. For the rf case the electron-particle reaction rate coefficients were assumed to follow the time variation of the applied sinusoidal field. These coefficients were averaged over a rf period and used in the chlorine density balance, Eq. (9). However, for the rf case, the time-dependent coefficients were used for the electron density balance, Eq. (5), with the auxiliary condition

$$\int_0^\tau \left(\frac{d}{dt} n_e\right) dt = 0, \tag{12}$$

to obtain a periodic steady state. Also a different form of the power balance was found to be more convenient for the rf case, namely,

$$\frac{P}{V_p} = \frac{1.6\times 10^{-36}}{\tau} \int_0^\tau E(t) v_d(t) n_e(t)\, dt, \tag{13}$$

where τ is the period of the applied field and $v_d(t)$ is the time-dependent drift velocity.

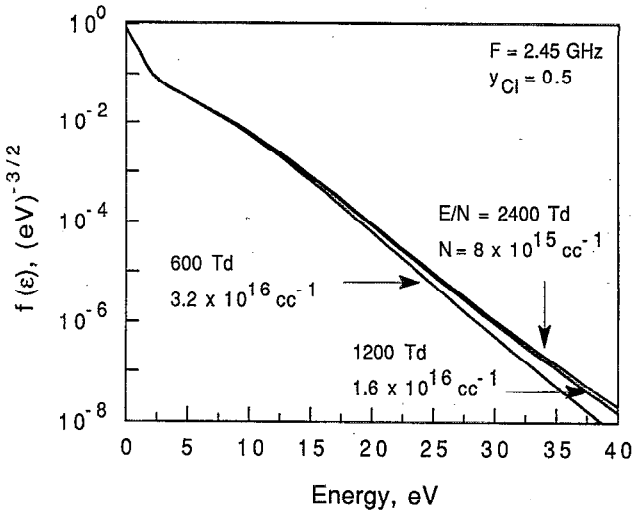

FIG. 3. Electron-energy distribution function for $F=2.45$ GHz, $y_{Cl}=0.5$, $E=192$ V/cm, and three different values of N (1 Td$=10^{-17}$ V cm^2).

IV. RESULTS AND DISCUSSION

A. Electron-energy distribution function

Results for the EEDF are presented here for the μW case. Results for the rf case were presented in Ref. 20. Figure 3 shows the normalized EEDF for $F=2.45$ GHz and 50% atomic chlorine, at three different (total) neutral number densities, but at the same applied field of rms value 192 V/cm. For this value of the rms field and for $N=3.2\times 10^{16}$/cm^3, $E_{rms}/N=600$ Td (1 Td$=10^{-17}$ V cm^2). As one goes to lower N, ν_m decreases and the criterion $\omega \gg \nu_m(\epsilon)$ is better satisfied [the average ν_m is about 4×10^9 s^{-1} at 3.2×10^{16}/cm^3], making the EEDF independent of E/N [see Eq. (1)], hence independent of N (for the constant E examined). A characteristic of the EEDF at high frequencies is a sharp rise in the population of low-energy electrons. This is because $\omega > \nu_m$ for the μW case examined here. Thus, although electrons gain energy from the applied field during one-half of the cycle, the field reverses its direction before electrons can undergo collisions. Consequently, electrons end up giving the acquired energy back to the field. This causes a higher population of low-energy electrons when compared to the rf case.

Figure 4 shows the effect of applied field intensity on the EEDF for a fixed gas composition and for $F=2.45$ GHz. As expected, the distribution shifts to higher electron energies at higher fields. Figure 4 also shows that the EEDF may be approximated by two Maxwellians (a Maxwellian distribution would be a straight line in the plot of Fig. 4). Thus the two-electron-group model[34] may be used to represent the system.

Figure 5 shows the dependence of the EEDF on gas composition at a fixed E/N and for $F=2.45$ GHz. As the mixture becomes richer in molecular chlorine the EEDF shifts to higher electron energies. This behavior is the opposite of that obtained for the rf case (see Aydil and Econ-

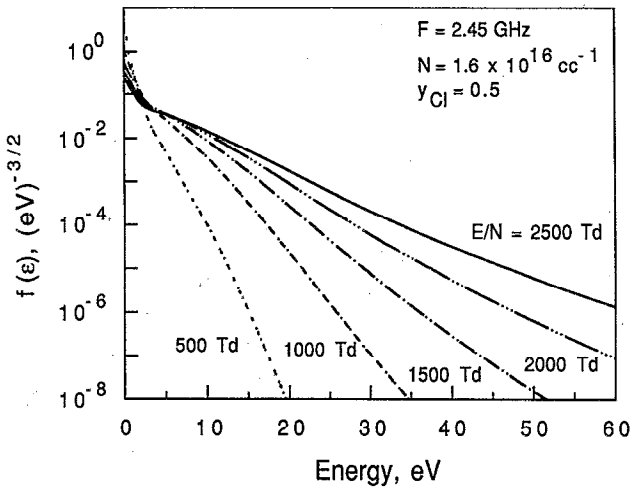

FIG. 4. Electron-energy distribution function for $F=2.45$ GHz, $y_{Cl}=0.5$, $N=1.6\times10^{16}/cm^3$, and different values of E/N.

omou[20]). It can be explained on the basis of the momentum exchange cross section for atomic and molecular chlorine using Eq. (1). Since $\nu_m(\epsilon)_{Cl_2}$ is larger than $\nu_m(\epsilon)_{Cl}$, the momentum exchange cross section $\nu_m(\epsilon)$ for a Cl_2/Cl mixture decreases as the fraction of Cl in the mixture increases. Let us now examine the quantity

$$\frac{\nu_m(\epsilon)E^2}{[\nu_m^2(\epsilon)+\omega^2]}=\frac{E_{\text{eff}}^2}{\nu_m(\epsilon)}, \tag{14}$$

which appears in the term containing the electric field in Eq. (1). Note that this quantity is proportional to the power supplied per electron by the field [Eq. (2)], and E_{eff} is the "effective electric field." For the μW case, $\omega>\nu_m(\epsilon)$ and this quotient decreases with decreasing $\nu_m(\epsilon)$ or

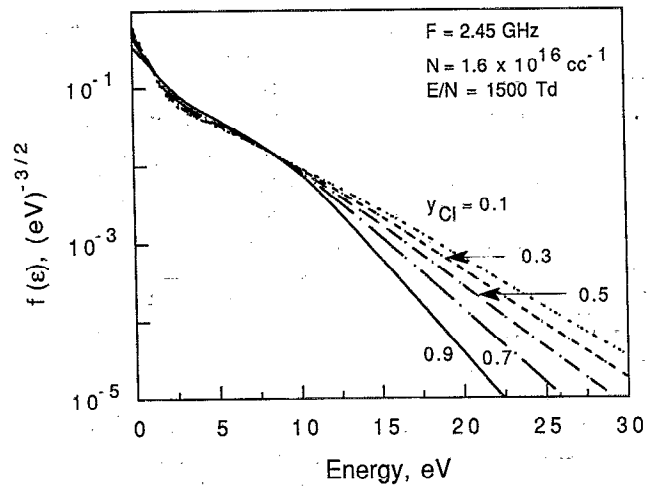

FIG. 5. Electron-energy distribution function for $F=2.45$ GHz, $E/N=1500$ Td, $N=1.6\times10^{16}/cm^3$, and different values of y_{Cl}.

TABLE II. Basic parameter values and range examined.

Name	Symbol	Basic value	Range
Tube radius	R	0.5 cm	0.5–1.0 cm
Excitation frequency	F	2.45 GHz and 13.56 MHz	N.D.
Neutral density	N	$1.6\times10^{16}/cm^3$	$0.8–3.2\times10^{16}/cm^3$
Feed flow rate	Q_0	5 sccm	1–100 sccm
Reaction probability	γ	4×10^{-5}	$0–4\times10^{-3}$
Power density	P/V_p	N.D.	0–10 W/cm^3
Length of plasma	L_p	10 cm	N.D.

equivalently with increasing Cl fraction in the mixture. When keeping E and ω constant (as in Fig. 5), a lower value of $\nu_m(\epsilon)$ is equivalent to a lower value of the field resulting in shorter tail of the EEDF. The opposite is true for the rf case because then $\omega<\nu_m(\epsilon)$ and the quotient of Eq. (14) increases with decreasing $\nu_m(\epsilon)$ (or equivalently with increasing Cl fraction in the mixture).

B. Plasma model

Basic parameter values and the range examined are shown in Table II. Equation (5) implies that the self-sustaining electric field will be established at a value such that the electron production rate by ionization equals the electron loss rate by attachment and diffusion. For small tube radii, the diffusion length Λ is correspondingly small [Eq. (8)], making diffusion the dominant electron loss mechanism.

Figure 6 shows the self-sustaining rms electric field and the corresponding ambipolar diffusion coefficient as a function of y_{Cl}. It can be seen that the rms field goes through a maximum as the mole fraction of atomic chlorine increases, whereas the diffusivity decreases monotonically. This behavior can be explained as follows: At low mole fractions of atomic chlorine the negative ion density greatly exceeds the electron density ($\alpha\gg1$) because of attachment to molecular chlorine. The space-charge fields are then

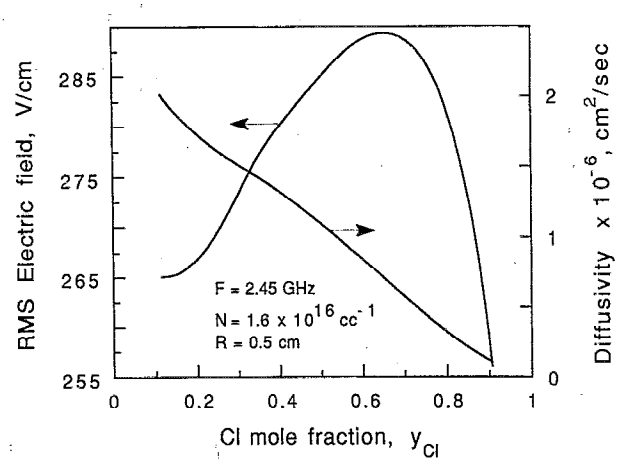

FIG. 6. Self-sustaining rms electric field and ambipolar diffusivity as a function of atomic chlorine mole fraction. $F=2.45$ GHz, $R=0.5$ cm, and $N=1.6\times10^{16}/cm^3$.

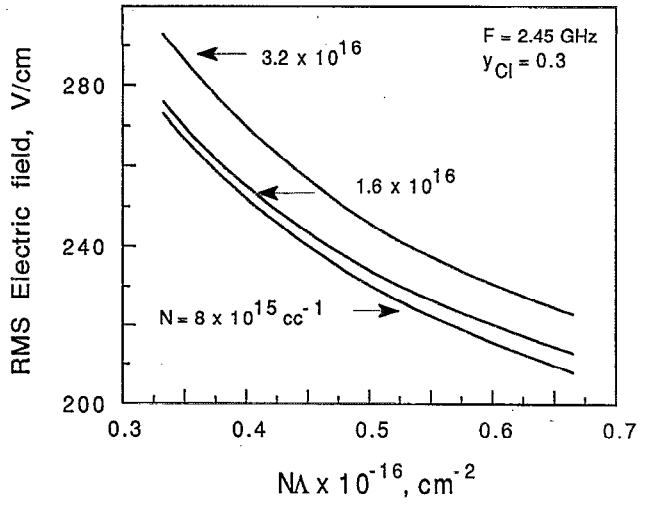

FIG. 7. Self-sustaining rms electric field as a function of $N\Lambda$ for three different N. F=2.45 GHz, y_{Cl}=0.3.

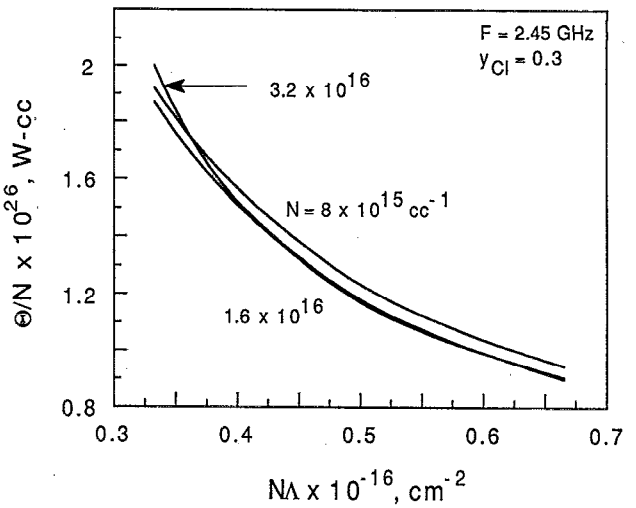

FIG. 8. Power per electron per neutral particle as a function of $N\Lambda$ for three different N. F=2.45 GHz, y_{Cl}=0.3.

greatly reduced and the electron diffusivity approaches its free value [see Eq. (6)]. As y_{Cl} increases, the discharge becomes less electronegative and the ambipolar diffusivity decreases. Now, the rms field is affected by y_{Cl} in two opposite ways: (a) As y_{Cl} increases the ambipolar diffusivity decreases and hence a lower field is required to sustain the discharge; and (b) as y_{Cl} increases the tail of the EEDF becomes shorter (Fig. 5), and the electric field has to increase to provide enough ionization to sustain the discharge. At low values of y_{Cl} effect (b) dominates over (a) whereas at high values of y_{Cl} effect (a) dominates over (b). The result is a maximum in the self-sustaining field at some intermediate value of y_{Cl}. This happens at an atomic chlorine mole fraction of about 0.65 as shown in Fig. 6. It should be noted that the power to the discharge is varied in Fig. 6 in order to achieve a given value of y_{Cl}.

Figure 7 shows the self-sustaining rms electric field as a function of $N\Lambda$. It is observed that the field decreases with increasing $N\Lambda$ since electron losses by diffusion decrease with increasing $N\Lambda$. Hence a lower field is sufficient to sustain the discharge. If attachment were the dominant electron loss mechanism, the E_{rms} would tend to become independent of $N\Lambda$. This should actually happen at sufficiently high values of $N\Lambda$, and is evident by the decreasing slope of the curves with increasing $N\Lambda$. One further observes that the rms field is not a unique function of $N\Lambda$ as would be predicted by the classical theory of the positive column.[34] Nevertheless the variations of E_{rms} with N (at constant $N\Lambda$) are relatively small. Figure 8 shows the power spent per electron and per neutral gas particle Θ/N as a function of $N\Lambda$. Here Θ is defined as the ratio of power density to electron density. Θ/N decreases with increasing $N\Lambda$ following the corresponding decrease in the rms field.

Figure 9 shows the atomic chlorine mole fraction obtained in the plasma as a function of power density for different gas flow rates at a constant neutral gas density. As expected, more molecular dissociation is achieved by increasing the power density delivered to the plasma. Very high degrees of dissociation are possible with only a few W/cm^3, especially at low flow rates. For a given power density, the mole fraction of atomic chlorine in the plasma decreases with increasing flow rate because the gas residence time in the plasma also decreases with flow rate. Hence the gas molecules have lower chance of dissociating as they flow through the plasma volume.

While the degree of gas dissociation affects the plasma characteristics through its effect on the EEDF, the atomic chlorine flux may be of greater practical importance. Figure 10 shows the atomic chlorine flux (flow rate Q_{Cl}) at the plasma exit as a function of inlet flow rate of molecular chlorine. Q_{Cl} was found using the relation

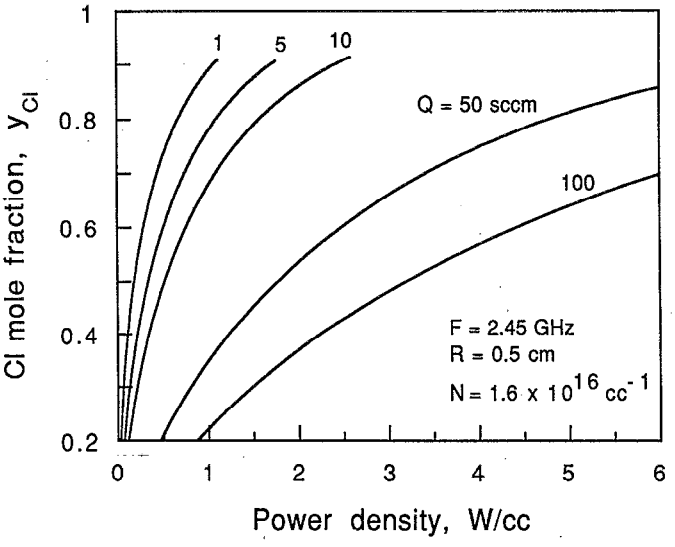

FIG. 9. Atomic chlorine mole fraction in the plasma as a function of power density, for different gas flow rates. F=2.45 GHz, R=0.5 cm, N=1.6×10^{16}/cm^3.

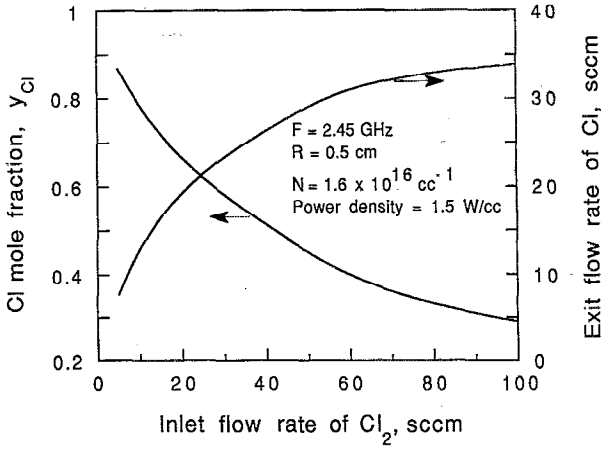

FIG. 10. Atomic chlorine mole fraction in the plasma (lhs axis) and flux out of the plasma (rhs axis) as a function of inlet gas flow rate. $F=2.45$ GHz, $R=0.5$ cm, $N=1.6\times10^{16}/\text{cm}^3$, and power density $=1.5$ W/cm^3.

$$Q_{Cl}=\frac{2y_{Cl}}{2-y_{Cl}}Q_0, \tag{15}$$

where Q_0 is the feed (Cl_2) flow rate. The atom flux increases with feed gas flow rate despite the fact that the degree of gas dissociation decreases with flow rate. Of course, for very high flow rates, the feed gas would spend very little time in the plasma and the atom mole fraction would then be vanishingly small. Thus one would expect a maximum in the atom flux with feed flow rate to be reached at a sufficiently high flow rate.

In the cases examined up to this point the wall recombination coefficient γ was taken to be 4×10^{-5}. Figure 11 shows the effect of changing γ. A higher γ value implies a larger drain for Cl atoms and hence a lower Cl concentration in the discharge. Of course, for too high values of γ,

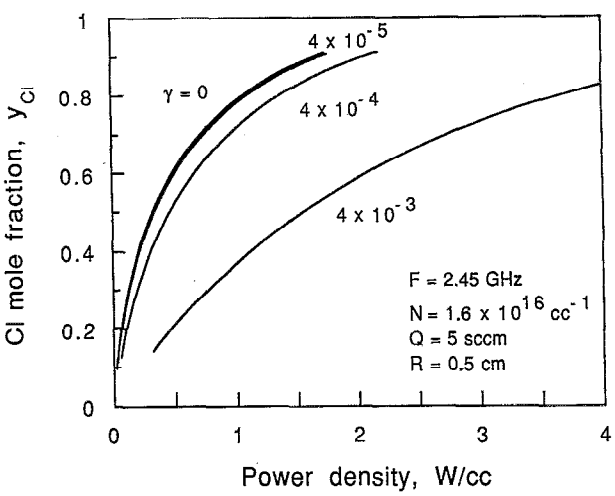

FIG. 11. Atomic chlorine mole fraction in the plasma as a function of power density for different wall recombination probabilities. $F=2.45$ GHz, $R=0.5$ cm, $N=1.6\times10^{16}/\text{cm}^3$, and $Q=5$ sccm.

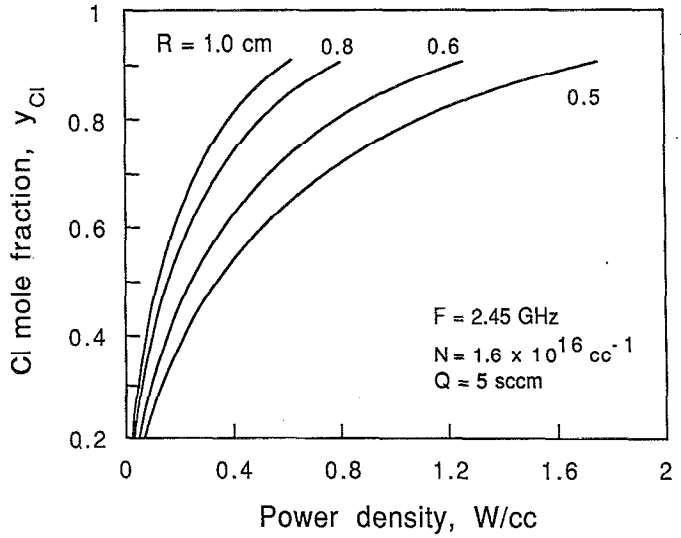

FIG. 12. Atomic chlorine mole fraction in the plasma as a function of power density for different tube radii. $F=2.45$ GHz, $N=1.6\times10^{16}/\text{cm}^3$, and $Q=5$ sccm.

significant atom concentration gradients set in and the assumption of a well-mixed reactor is violated. Figure 11 also shows that wall recombination is not an important atom loss mechanism so long as γ is less than a few times 10^{-4}.

Figure 12 shows the effect of tube radius. For a given power density, more dissociation is obtained by using a larger tube radius. This is because as tube radius increases the plasma volume increases as well and the gas residence time in the plasma increases correspondingly (note that the comparison is made at constant flow rate). Also, electron diffusion losses decrease with increasing tube radius and this results in higher electron density. However, the electron energy (and hence k_d) decreases since the E_{rms} decreases (see Fig. 9). It should be noted that the power delivered to the plasma must be increased to maintain the same power density as tube radius increases.

The effect of neutral number density N at fixed input power can be seen in Fig. 13. As neutral density increases the number of Cl_2 molecules available for dissociation increases, but volume recombination increases faster. The result is greater dissociation at lower N, for a given power density.

For typical conditions ($N=1.6\times10^{16}/\text{cm}^3$, $R=0.5$ cm, $F=2.45$ GHz) the electron density ranged from $\sim10^8/\text{cm}^3$ for low Cl mole fractions (~0.1) to $\sim2\times10^{10}/\text{cm}^3$ for high Cl mole fractions (~0.9). The corresponding negative ion density ranged from $\sim7\times10^{10}/\text{cm}^3$ to $\sim4\times10^{11}/\text{cm}^3$. Under these conditions the ratio of electron to neutral particle density is $<10^{-5}$.

C. Comparison between rf and microwave discharges

For the base case of $R=0.5$ cm, $Q=5$ sccm, and $N=1.6\times10^{16}/\text{cm}^3$, Fig. 14 shows the extent of dissociation that can be obtained as a function of power density for the two frequencies considered in this work. It can be seen that

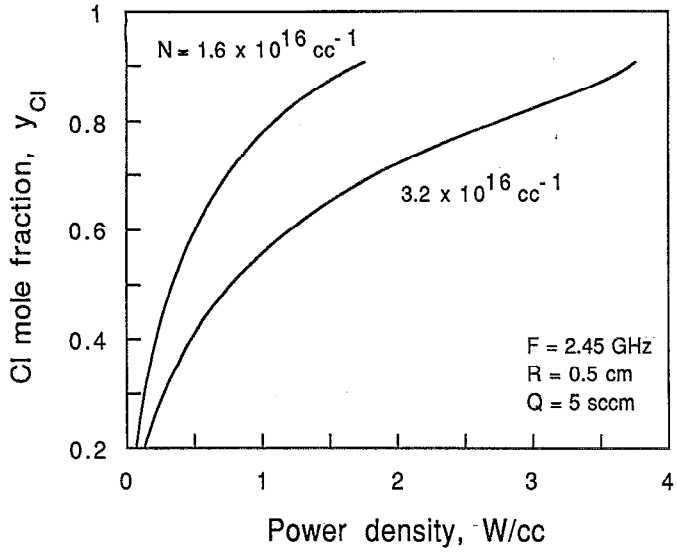

FIG. 13. Atomic chlorine mole fraction in the plasma as a function of power density for two different N. F=2.45 GHz, R=0.5 cm, and Q=5 sccm.

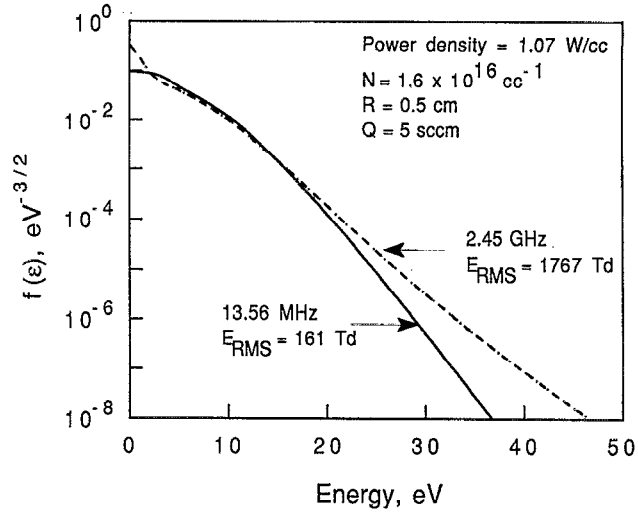

FIG. 15. Electron-energy distribution function for the self-sustaining discharge operating under the conditions of Fig. 14 with a power density of 1.07 W/cm^3 (this corresponds to y_{Cl}=0.8).

similar levels of dissociation can be obtained for the two cases. The electron densities were also found to be comparable and so the power required to sustain an electron-ion pair is similar for the two frequencies. Several other sets of operating conditions were also analyzed, and the degree of gas dissociation was found not to differ significantly at the two frequencies.

In order to explain this weak frequency dependence, the situation corresponding to a Cl mole fraction of 0.8 is analyzed in greater detail. The self-sustaining rms electric field for the two frequencies is E_{rf}=25.76 V/cm and $E_{\mu w}$ =282.7 V/cm. The effective collision frequency for the μW case is 1.33×10^9 s^{-1} and this gives an equivalent effective dc field of E_{eff}=24.3 V/cm [using Eq. (14)]. For the rf case the effective field will be same as the rms field, i.e., 25.76 V/cm, since $\nu_m \gg \omega$. It is seen that the values of the effective field for the two frequencies are close to one another.

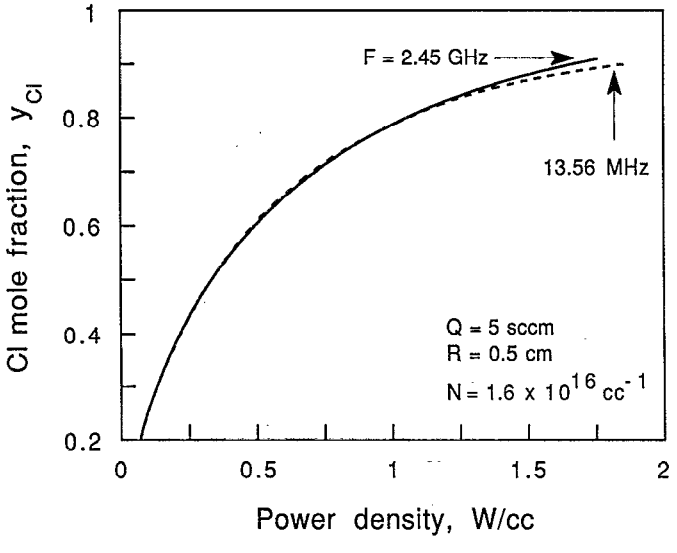

FIG. 14. Atomic chlorine mole fraction in the plasma as a function of power density for two different frequencies. R=0.5 cm, $N=1.6\times10^{16}$/cm^3, and Q=5 sccm.

Figure 15 shows the distribution functions under these conditions. The EEDF at 13.56 MHz was calculated as the dc distribution that would be obtained at the rms value of the actual self-sustaining electric field. This was thought to be representative of an average of the true time-dependent distribution. The two EEDF nearly coincide in the range 4–16 eV. This range of electron energies is most important for production of atomic chlorine by dissociative excitation. Electrons with energy less than 3.12 eV are below the dissociative excitation threshold, and there are only very few electrons with energy above 16 eV contributing to dissociation. The relevant rate coefficient k_d for the μW, time-averaged rf and dc evaluated at E_{rms}=25.76 V/cm cases were found to be 1.21×10^{-8}, 1.18×10^{-8}, and 1.39×10^{-8} cm^3/s, respectively. These values do not differ enough from one another to cause a significant difference in atomic chlorine mole fraction (the values for k_a were even closer to one another). It should be emphasized that the rate coefficients for other processes (a process with threshold greater than 20 eV for instance) can differ significantly under the same conditions. Also, the comparison at the two frequencies was done at constant power.

Experimental data comparing the degree of gas dissociation in chlorine discharges at rf and microwave frequencies could not be found. The difficulty is that all variables except frequency must be kept constant for a meaningful comparison to be made; however, data on oxygen discharges suggest similar degrees of gas dissociation at 13.56 MHz and 2.45 GHz.[7] Nevertheless, direct comparison is difficult to make because all other conditions were not kept

the same (for example the reactor geometry was different). Our experiments with a 2.45 GHz chlorine discharge were recently completed. Data on the chlorine mole fraction as a function of applied power are in good agreement with the model predictions.[35]

Recently, Karoulina and Lebedev[36] compared a dc with a microwave argon discharge. They concluded that the rates of excited species production in the two discharges are the same as long as one keeps the same tube radius, pressure, power, and wall temperature. The same conclusion is reached in our study by comparing a rf with a microwave chlorine discharge.

At this point it is appropriate to comment on the assumption that the EEDF follows the applied field in the rf case. The energy relaxation frequency ν_u, can be approximated by $\nu_u = \nu_d E/\epsilon_k$, where ϵ_k is the characteristic energy of the electrons. For the situation discussed above, the drift velocity at the rms field is 3.7×10^7 cm/s and the electron characteristic energy is 4.7 eV. The energy relaxation frequency turns out to be 2×10^8 s^{-1}, more than twice the applied angular frequency of $\omega = 8.52\times10^7$ rad/s. Rogoff and co-workers[19] have provided a plot of the self-sustaining electric field versus pressure which gives the minimum field that is necessary at a given pressure for the condition $\nu_u > \omega$ to hold.

V. SUMMARY AND CONCLUSIONS

A mathematical model was developed for the bulk plasma of an electrodeless chlorine discharge sustained in a tubular reactor. The plasma may be excited at radio frequencies (rf, commonly at 13.56 MHz) by inductive coupling or at microwave frequencies (μW, commonly at 2.45 GHz) by a resonant cavity. The model consisted of balance equations for calculating the self-sustaining electric field, electron density, and atomic chlorine density in the plasma. Electron transport properties and rate coefficients of electron-particle (atom or molecule) reactions were obtained by solving the Boltzmann transport equation for the electron-energy distribution function (EEDF). The effect of chlorine atoms (resulting from dissociation of molecular chlorine) on the EEDF was taken into account. The effect of frequency, power, gas feed rate, tube radius, and wall recombination coefficient on the chlorine atom density in the plasma was investigated. In particular two extreme excitation frequencies were examined: 13.56 MHz at which the EEDF was assumed to follow the variations of the field, and 2.45 GHz at which the EEDF cannot follow the field. The results can be summarized as follows:

(i) Discharges at 13.56 MHz and 2.45 GHz gave nearly the same atom density, under otherwise identical conditions (e.g., same power). This was explained by the fact that the EEDF at the two frequencies were nearly the same in the range of electron energies (4–16 eV) which is most important for producing chlorine atoms.

(ii) Almost complete dissociation of the molecular gas can be attained with only a few W/cm^3 of power delivered to the plasma.

(iii) Despite the fact that the atom density in the plasma decreases as the feed gas flow rate increases, the atom flux increases with flow rate. Hence higher flow rates favor higher atom fluxes but the gas utilization is correspondingly lower.

(iv) Lower gas pressure, larger tube radius, and lower wall recombination material favor higher atom densities. For the conditions examined, wall recombination was not an important sink of chlorine atoms as long as the wall recombination reaction probability was lower than a few 10^{-4}.

Practical reactors have a plasma region which serves as the source of radicals and a downstream region through which the radicals flow (and perhaps mixed with other gases) before impinging on the substrate. The ultimate goal is to maximize the flux of beneficial radicals on the substrate. Hence, in addition to the factors affecting radical density in the plasma, transport and reaction of these radicals in the downstream region must be considered. Preliminary results indicate that lower pressure and higher flow rate result in higher atom flux not only at the plasma exit but also at the end of the downstream section (see Fig. 1). A conflict may arise in choosing the tube radius. Under otherwise identical conditions, a tube with larger radius in the plasma region than in the downstream region may yield higher radical flux. These findings are qualitatively similar to the ones reported in a study of transport and reaction in a plasma assisted downstream etching system.[37] In that earlier work a rudimentary treatment of the plasma (radical source) region was adopted. Rather detailed models of the plasma, such as the one developed here, can be used as "modules" in multidimensional radical transport and reaction models of remote plasma processing reactors. The latter will yield quantitative predictions of etch or deposition rate, and would be useful for identifying reactor designs and the window of operating conditions for optimum performance.

ACKNOWLEDGMENT

This work was supported by the State of Texas through the Texas Center for Superconductivity at the University of Houston.

[1] D. M. Manos and D. L. Flamm, Eds., *Plasma Etching: An Introduction* (Academic, New York, 1989).
[2] G. Lucovsky, D. V. Tsu, and R. J. Markunas, in *Handbook of Plasma Processing Technology*, edited by S. M. Rossnagel, J. J. Cuomo, and W. D. Westwood (Noyes, Park Ridge, NJ, 1990).
[3] V. Vukanovic, G. A. Takacs, E. A. Matuszak, F. D. Egitto, F. Emmi, and R. S. Horwath, J. Vac. Sci. Technol. B **6**, 66 (1988).
[4] M.-C. Chuang and J. W. Coburn, J. Vac. Sci. Technol. A **8**, 1969 (1990).
[5] G. Lucovsky, P. D. Richard, D. V. Tsu, S. Y. Lin, and R. J. Markunas, J. Vac. Sci. Technol. A **4**, 681 (1986).
[6] N. Selamoglu, J. A. Mucha, D. E. Ibbotson, and D. L. Flamm, J. Vac. Sci. Technol. B **7**, 1345 (1989).
[7] M. J. Kushner, J. Appl. Phys. **71**, 4173 (1992).
[8] S. W. Choi, G. Lucovsky, and K. J. Bachmann, J. Vac. Sci. Technol. B **10**, 1070 (1992).
[9] J. Kuo, M. Hong, D. J. Trevor, R. M. Flemming, A. E. White, R. C. Farrow, A. R. Kortran, and K. T. Short, Appl. Phys. Lett. **53**, 2683 (1988).
[10] D. L. Flamm, J. Vac. Sci. Technol. A **4**, 729 (1986).
[11] A. T. Bell and K. Kwong, AIChE J. **18**, 990 (1972); Ind. Eng. Chem. Fundam. **12**, 90 (1973).

[12] M. Moisan, C. Barbeau, R. Claude, C. M. Ferreira, J. Margot, J. Paraszczak, A. B. Sa, G. Sauve, and M. R. Wertheimer, J. Vac. Sci. Technol. B **9**, 8 (1991).
[13] M. L. Passow, M. L. Brake, P. Lopez, W. B. McColl, and T. E. Repetti, IEEE Trans. Plasma Sci. **PS-19**, 219 (1991).
[14] D. A. Danner and D. W. Hess, J. Appl. Phys. **59**, 940 (1986).
[15] W. Denneman, J. Phys. D **23**, 293 (1990).
[16] G. G. Lister and M. Cox, Plasma Sources Sci. Technol. **1**, 67 (1992).
[17] T. Makabe and N. Goto, J. Phys. D **21**, 887 (1988).
[18] C. Ferreira, L. L. Alves, M. Pinheiro, and A. B. Sa, IEEE Trans. Plasma Sci. **PS-19**, 229 (1991).
[19] G. L. Rogoff, J. M. Kramer, and R. B. Piejak, IEEE Trans. Plasma Sci. **PS-14**, 103 (1986).
[20] E. S. Aydil and D. J. Economou, J. Electrochem. Soc. **139**, 1396 (1992); **139**, 1406 (1992).
[21] P. E. Luft, Joint Inst. for Lab. Astrophysics, Univ. of Colorado, Boulder, Report 14, 1975.
[22] W. P. Allis, *Handbook of Physics* (Wiley, New York, 1956), Vol. 21, p. 404; D. J. Rose and S. C. Brown, Phys. Rev. **98**, 310 (1955).
[23] C. M. Ferreira, in *Radiative Processes in Discharge Plasmas*, edited by J. M. Proud and L. H. Luessen, NATO ASI Series B, Physics, Vol. 149 (Plenum, New York, 1985), p. 431.
[24] L. L. Alves and C. M. Ferreira, J. Phys. D **24**, 581 (1991).
[25] S.-K. Park and D. J. Economou, J. Appl. Phys. **68**, 3904 (1990).
[26] H. Massey, *Negative Ions* (Cambridge University Press, London, 1976).
[27] C. H. Muller and A. V. Phelps, J. Appl. Phys. **51**, 6141 (1980).
[28] G. L. Rogoff, J. Phys. D **18**, 1533 (1985).
[29] D. K. Davies, Air Force Wright Aeronautical Labs., Wright-Patterson Air Force Base, Dayton, OH, Final Report AFWAL-JR-82-2083, 1982.
[30] M. J. Church and D. Smith, J. Phys. D **11**, 2199 (1978).
[31] E. A. Ogryzlo, Can. J. Chem. **39**, 2556 (1961).
[32] A. C. Lloyd, Int. J. Chem. Kinet. **3**, 39 (1971).
[33] M. Kubicek, ACM Trans. Math. Software **2**, 98 (1976).
[34] B. E. Cherrington, *Gaseous Electronics and Gas Lasers* (Pergamon, Oxford, 1979).
[35] S. C. Deshmukh and D. J. Economou (unpublished).
[36] E. V. Karoulina and Yu A. Lebedev, J. Phys. D **25**, 401 (1992).
[37] S.-K. Park and D. J. Economou, J. Appl. Phys. **66**, 3256 (1989).